

# Observational Tests of Gauss-Bonnet Like Dark Energy Model

Z. Molavi <sup>\*</sup> and A. Khodam-Mohammadi <sup>†</sup>

*Department of Physics, Faculty of Science,  
Bu-Ali Sina University, Hamedan 65178, Iran*

## Abstract

The consistency of some dynamical dark energy models based on Gauss-Bonnet invariant,  $\mathcal{G}$ , is studied compared with cosmological observational tests. The investigated models are modified form of Gauss Bonnet dark energy, MGB-DE and two other versions which are interacting MGB and  $n_0$ MGB. The energy density of proposed models are combinations of powers of the Hubble rate,  $H$ , and its time derivative. To inquire the performance of MGB dark energy models, we have used data analyzing methods and numerical solutions, in both background and perturbed levels, based on recent observational data from SNIa, Baryon Acoustic Oscillations (BAO), Hubble parameter, CMB data, and structure formation data surveys. Employing joint data sets and comparing the results to those of  $\Lambda$ CDM, show that all versions of MGB-DE predicts the expansion history and evolution of structures appropriately as well as  $\Lambda$ CDM. If we use pure late universe data set, we see that all models of MGB-DE are successful in recent epoch, and there is not any significant evidence against or in favor of  $\Lambda$ CDM, whereas for early universe, statistical results indicate a significantly better agreement for  $\Lambda$ CDM as compared to all versions of MGB-DE models.

---

<sup>\*</sup> Email:zmolavi26@gmail.com

<sup>†</sup> Email:khodam@basu.ac.ir (corresponding author)

## I. INTRODUCTION

Entering the era of precision cosmology, scientists faced huge amount of data, received by several surveys from the mysterious sky. The accurate astrophysical data from distant Ia supernovae [1], [2], [3], cosmic microwave background anisotropy [4], [5], and large scale galaxy surveys [6], [7], reveals that the universe is nearly spatially flat and is definitely passing an accelerating expansion phase. This is one of the most fundamental concepts in theoretical cosmology and particle physics.

During last decades, quite high number of models have been presented in this context. These models are mainly categorized in two classes. The first insists on modifying and extending the gravity itself, named modified gravity. Modified gravity models assume that, the present accelerating epoch is due to geometric effects and corresponds to modify General Relativity, by modifying the Einstein-Hilbert action. Modification of GR, subsequently, leads to new formulation in gravity. The models in this class are  $f(R)$  and  $f(T)$  gravity [8–17], scalar-tensor theories [18], braneworld models [19–22] Gauss-Bonnet gravity [23–26] and so on.

Other category is based on presence of an exotic component in stress energy tensor, with sufficiently negative-pressure. This fluid which is known as dark energy, accounts for roughly 75 percent of the universe energy density today. Big variety of dark energy models are proposed, nevertheless the nature and mechanism of dark energy is not known yet. One of the most famous models, vastly used in literature, is cold dark matter plus a cosmological constant named ( $\Lambda$ CDM) model. It explains the scenario of acceleration of the universe and has an acceptable compatibility with recent observational data [27], [28], [29], [30]. However this model suffers from distinct problems; Fine tuning and coincidence. This made theorists seek for some dynamical models instead [10, 31]. Actually any offered dark energy model must entail all aspects of quantum theory, particle physics and general relativity. One approach is holographic principle, according to which, the entropy of a system scales not with its volume but with its surface area [32, 33]. The motivation for this, was first arisen from Bekenstein's entropy bound,  $S \leq \pi M_p^2 L^2$ , from which it is implied that in entropies well below this bound, quantum field theory fails. Imposing a relation between UV and IR cut-offs, as indicated in [34], conciliated this problem. This relationship was established by using the limit set by black hole formation, that is  $L^3 \Lambda^4 \leq \pi M_p^2 L^2$  where  $M_p$  is the reduced Planck mass. A holographic DE model where the IR cut-off is given by the Ricci scalar and

the Gauss-Bonnet (GB) invariant was proposed in [35].

Recently, many dynamical DE models, against rigid concordance model ( $\Lambda$ CDM), has been proposed. The energy density of these models composed of terms like  $\dot{H}$ ,  $H\dot{H}$ ,  $H^2$  etc., which are studied in many papers, e.g. [36, 37] and the role of terms like  $H^3$ ,  $\dot{H}H^2$  and  $H^4$  in the evolution of early universe has been investigated [38–42]. It is worthwhile to mention that in one form of these models ( $\rho_D = C_0 + C_1H^2 + C_2\dot{H}$ ), authors concluded that their model indicate a significantly better agreement with observations as compared to the concordance  $\Lambda$ CDM model [43].

The studied model in present paper has been firstly proposed by [44], named natural scaling for DE, so that we called it latter by Gauss-Bonnet DE model [45]. It complies the holographic principle and obeys the above bound for black hole formation. The related energy density is proportional to the Gauss-Bonnet 4-dimensional invariant,  $\mathcal{G}$ , in such a way that it has the valid dimension of energy density [44]. This invariant is used in corrections of low energy string gravity. The GB-DE energy density is composed of powers of Hubble parameter and its derivative. Many authors have used the GB term in the bulk, coupled with some scalar fields or DE models [46–48]. Also the reconstruction of the holographic DE in the framework of the modified GB gravity was performed in [49] and other applications of the GB gravity in the context of the holographic principle have been studied in [50–52]. Moreover the GB term is employed in dark energy context with different forms in the action, like coupled to some scalar field, used in modified theories [23–26], or as modified dark energy models as in [45, 53]. Specially authors in [45], showed that only modified GB-DE has capability to have stability against the density perturbation. The investigation of the cosmic evolution and the compatibility with the observations can help us to judge about GB-DE models.

This paper is organized as follows: In Sec.II, we review the Gauss-Bonnet universe, in background and perturbations point of views. In Sec.III, we proceed to data analysis and the results of these methods for our models and at last finished our work with some concluding remarks.

## II. THE GAUSS-BONNET UNIVERSE

### A. Background equations

The energy density of GB-DE has been firstly introduced by [53]

$$\rho_d = \alpha \mathcal{G}, \quad (1)$$

where  $\alpha$  is a dimensionless parameter and  $\mathcal{G}$  is the 4-dimensional Gauss-Bonnet invariant which is defined as

$$\mathcal{G} = R^2 - 4R_{\mu\nu}R^{\mu\nu} + R_{\mu\nu\eta\gamma}R^{\mu\nu\eta\gamma}. \quad (2)$$

It's easy to see that for the flat FRW background,  $ds^2 = -dt^2 + a(t)^2 \sum_{i=1}^3 (dx^i)^2$ , the GB dark energy density (1) can be written as

$$\rho_d = 24\alpha \left( H^4 + H^2 \dot{H} \right). \quad (3)$$

### Modified Gauss-Bonnet Dark energy

Modified GB-DE (MGB-DE) has the following energy density [44]

$$\rho_d = \gamma H^4 + \beta H^2 \dot{H}, \quad (4)$$

with two independent free parameter  $\gamma$  and  $\beta$ . For a single component universe (in the absence of matter), the Friedmann equation with the energy density given by (2), in the flat FRW background takes the form

$$\beta \frac{dH}{dt} + \gamma H^2 - \frac{3}{\kappa^2} = 0, \quad (5)$$

where  $\kappa^2 = 8\pi G = M_p^{-2}$ . With suitable initial condition, this equation is solved and discussed in [44].

In presence of matter (baryonic and dark), the Friedmann equation becomes non-linear and does not have exact solution. Adding the matter term  $\rho_m = (\rho_c + \rho_b) = \rho_{m0} a^{-3}$ , the Friedmann equation reads

$$a\tilde{\beta}E^3E' - E^2 + \tilde{\gamma}E^4 + \frac{\Omega_m}{a^3} = 0 \quad (6)$$

where  $\tilde{\gamma} = \kappa^2 H_0^2 \gamma / 3$ ,  $\tilde{\beta} = \kappa^2 H_0^2 \beta / 3$  and  $\Omega_{m0} = \kappa^2 \rho_{m0} / (3H_0^2)$  ( $\Omega_m = \kappa^2 \rho_m / (3H^2)$ ). The scaled Hubble parameter is defined as  $E = H/H_0$ . With the initial condition,  $E(1) = 1$ , and

different amounts of parameters, this equation could be solved numerically.

Since we are interested in late universe data or their mixture with those of background solutions in recent time, we can neglect radiation in the evolutionary equations.

### **The Interacting MGB model**

The interacting MGB (IMGB) model of DE is also introduced as a second model. Dark energy models in GR, suffer from the coincidence problem referred to energy density orders of dark matter and dark energy. This problem could be solved by assuming continuous energy exchange between dark sectors. The signature of non-gravitational interaction term  $\bar{Q}$ , in the continuity equations, shows the direction of energy transfer

$$\dot{\bar{\rho}}_c + 3H\bar{\rho}_c = \bar{Q}, \quad (7)$$

$$\dot{\bar{\rho}}_d + 3H(1+w)\bar{\rho}_d = -\bar{Q}. \quad (8)$$

Here  $w = \bar{P}_d/\bar{\rho}_d$ . The  $\bar{Q}$  as the rate of energy density transfer is usually introduced as

$$\bar{Q} = -(\Gamma_m\bar{\rho}_m + \Gamma_d\bar{\rho}_d) \quad (9)$$

where  $\Gamma_i$ 's ( $\Gamma_m$  or  $\Gamma_d$ ) are constant energy density transfer rates and show the decay of dark matter to dark energy, or vice versa (Baryons (b) and photons ( $\gamma$ ) are not coupled to dark energy). We are interested in the special case  $\Gamma_d = 0$  and choose  $\Gamma_m = 3H\xi^2$ . Hence from the continuity equation, the dark matter density is

$$\bar{\rho}_m = \rho_{0m}a^{-3(1-\xi^2)} \quad (10)$$

and also the Eq. (6) changes to

$$a\tilde{\beta}E^3E' - E^2 + \tilde{\gamma}E^4 + \frac{\Omega_b}{a^3} + \frac{\Omega_c}{a^{3(1-\xi^2)}} = 0. \quad (11)$$

### **MGB with a constant**

As a third model, we consider the MGB with an arbitrary constant like the approach in [37] and [54]. For this, we added a constant  $n_0$  to the Eq. (6) directly. It is worth noting that for a very small value of  $H(z)$ , it reduced to familiar  $\Lambda$ CDM model.

$$a\tilde{\beta}E^3E' - E^2 + \tilde{\gamma}E^4 + \frac{\Omega_m}{a^3} + n_0 = 0. \quad (12)$$

## B. The linear perturbed equations

In perturbation theory, we consider a perturbed spacetime that is close to the background spacetime. This means that there exists a coordinate system on the perturbed spacetime, where its metric can be written as

$$g_{\mu\nu} = \bar{g}_{\mu\nu} + \delta g_{\mu\nu}. \quad (13)$$

Here  $\bar{g}_{\mu\nu}$  is the metric of the background. Thus metric perturbations are divided into a scalar, vector and a tensor part, which do not couple to each other in first-order perturbation theory and evolve independently. Scalar perturbations are of special importance. They couple to density and pressure perturbations and cause gravitational instabilities. This make overdensities grow and become more overdense. The outcome is formation and growth of Large Scale Structure (LSS), from small initial perturbations. In order to study the linear perturbation theory, we start with perturbation equations. In the perturbed FRW universe, with scalar perturbations and in absence of anisotropic stress, the line element is

$$ds^2 = -(1 + 2\Phi)dt^2 + a^2(t)(1 - 2\Psi)d\vec{x}^2, \quad (14)$$

where  $\Phi$  and  $\Psi$  are metric perturbations known as the Bardeen potentials. Perturbations in density (matter or energy) and pressure are

$$\rho = \bar{\rho} + \delta\rho \quad (15)$$

$$p = \bar{p} + \delta p \quad (16)$$

where  $\bar{p}$  and  $\bar{\rho}$  are pressure and density of background. The perturbed energy momentum tensor is

$$T^\mu_\nu = \bar{T}^\mu_\nu + \delta T^\mu_\nu \quad (17)$$

The DE component is expected to be smooth and we consider perturbations only on the matter component of the cosmic fluid. The energy-momentum continuity equation needs  $T^\mu_{\nu;\mu} = 0$ . In absence of interaction between dark matter and dark energy and in Fourier space this equation leads to

$$\dot{\delta}_m = (1 + \omega_m)(3\dot{\Psi} + \frac{k}{a}\theta_m), \quad (18)$$

$$\dot{\theta}_m + (1 - 3\omega_m)H\theta_m = \frac{k}{a}(\Phi + \frac{\omega_m}{1 + \omega_m}\delta_m), \quad (19)$$

in which  $\delta_m (= \delta\rho_m/\rho_m)$  is dark matter density contrast and  $\theta_m$  is the divergence of velocity field. We are interested in the case of non-relativistic fluid ( $\omega_m = 0$ ) and scales much smaller than Hubble radius ( $k \gg aH$ ). So that the above equations result into a second order differential equation, for evolution of matter density contrast. In terms of scale factor it reads

$$\delta_m'' + \left( \frac{3}{a} + \frac{E'}{E} \right) \delta_m' - \frac{3}{2a^2 E^2} \Omega_m \delta_m = 0. \quad (20)$$

For coupled MBG dark energy, the changes are exhibited in the background evolution equations, in  $\Omega_m$  term.

Solving the system of equations (6) and (20) gives the evolution of density contrast for the models. In order to study structure formation and compare models with data, it is needed to use some definitions. The first concept is the growth rate function defined with the following equation

$$f(a) = \frac{d \ln \delta_m}{d \ln a}. \quad (21)$$

The observable that we need to measure in structure formation context, is  $f\sigma_8$ , in which,  $\sigma_8$  is

$$\sigma_8(a) = \sigma_{8,0} \frac{\delta_m(a)}{\delta_0} \quad (22)$$

where  $\delta_0$  is the density contrast in  $a = 1$ .

Another important quantity we can refer to is the  $\gamma$ -index. This index is related to matter perturbations and is defined via  $f(z) \simeq \Omega_m(z)^{\gamma(z)}$ , so the growth index  $\gamma(z)$  can be written as

$$\gamma(z) \cong \frac{\ln f(z)}{\ln \Omega_m(z)} \quad (23)$$

### III. OBSERVATIONAL CONSTRAINTS

In this section we use data analyzing methods in order to find the best fit values of the parameters in background and perturbed level for MGB-DE universe. To study the expansion history and the growth rate of structures, we ought to define some observables at first. The most important are the background expansion indicators such as distance modulus of Supernovae type Ia, Hubble parameter, Baryon acoustic oscillations (BAO) and CMB power spectrum. The observable related to perturbation growth rate of structures is  $f\sigma_8$  data and is taken into account correspondingly.

The respective parameters to be defined are: parameters of the MGB-DE models,  $\tilde{\beta}, \tilde{\gamma}, \xi, n_0$  plus usual cosmological parameters like current matter and baryon density parameters,  $\Omega_m^0$ ,  $\Omega_b^0$  and  $h = H_0/100$  (normalized Hubble constant).

Available observational data sets, used for these calculations are: distance modulus of Supernovae Type Ia, Baryon acoustic oscillations (BAO), Hubble evolution data, growth rate data  $f\sigma_8$  and WMAP data for CMB which will be explained;

### A. observables

The main evidence for cosmic accelerated expansion is Supernovae. Measuring the luminosity distance of these objects not only gives useful information about history of early universe but also constrain model parameters in low and intermediate redshifts confidently. Referred catalogue is the SnIa distance module from Union 2.1 sample [55], which includes 580 SnIa over the redshift range  $0 < z < 1.4$ .

By introducing covariant matrix  $\mathbf{C}_{\text{sn}}$ , which includes systematic uncertainties and correlation information of SNIa data sets, from [55], the  $\chi^2$  for SnIa is given by:

$$\chi_{\text{SN}}^2 = \mathbf{U}^T \mathbf{C}_{\text{sn}}^{-1} \mathbf{U} , \quad (24)$$

in which

$$\mu_{\text{th}}(z) = 5 \log_{10} \left[ (1+z) \int_0^z \frac{dx}{E(x)} \right] + \mu_0, \quad (25)$$

and

$$\mathbf{U} = \mu_{\text{th}}(z_i) - \mu_{\text{ob}}(z_i) \quad (26)$$

are the theoretical distance modulus and the difference matrix  $\mathbf{U}$ , accordingly. Because of applying covariance matrix  $\mathbf{C}_{\text{sn}}$  we do not regard the noisy parameter  $\mu_0$ . Baryon acoustic oscillations (BAO), are the imprint of oscillations in the baryon-photon plasma on the matter power spectrum. They are less affected by nonlinear evolution so they can be used as a standard ruler. The BAO data can be applied to measure the angular diameter distance  $D_A$  and the expansion rate of the Universe  $H(z)$  either separately or through the combination. We utilize 6 reliable measurements of BAO indicator, including Sloan Digital Sky Survey (SDSS) data release, 7 (DR7), SDSS-III Baryon Oscillation Spectroscopic Survey (BOSS), WiggleZ survey and 6dFGS survey. BAO observations contain measurements from redshift interval,  $(0.1 < z < 0.7)$ , summarized in Table.I. The  $\chi$  square for BAO, as mentioned in



Redshift	Data Set	$r_s/D_V(z; \{\Theta_p\})$	Ref.
0.10	6dFGS	$0.336 \pm 0.015$	[56]
0.35	SDSS-DR7-rec	$0.113 \pm 0.002$	[57]
0.57	SDSS-DR9-rec	$0.073 \pm 0.001$	[58]
0.44	WiggleZ	$0.0916 \pm 0.0071$	[59]
0.60	WiggleZ	$0.0726 \pm 0.0034$	[59]
0.73	WiggleZ	$0.0592 \pm 0.0032$	[59]

TABLE I: Observed data for BAO [60].

[60], is

$$\chi_{\text{BAO}}^2 = \mathbf{Y}^T \mathbf{C}_{\text{BAO}}^{-1} \mathbf{Y} , \quad (27)$$

where  $\mathbf{Y} = (d(0.1) - d_1, \frac{1}{d(0.35)} - \frac{1}{d_2}, \frac{1}{d(0.57)} - \frac{1}{d_3}, d(0.44) - d_4, d(0.6) - d_5, d(0.73) - d_6)$  and

$$d(z) = \frac{r_s(z_{\text{drag}})}{D_V(z)} , \quad (28)$$

with

$$r_s(a) = \int_0^a \frac{c_s da}{a^2 H(a)} , \quad (29)$$

where  $r_s(a)$  is the comoving sound horizon at the baryon drag epoch,  $c_s$  is the baryon sound speed and  $D_V(z)$  is defined by:

$$D_V(z) = \left[ (1+z)^2 D_A^2(z) \frac{z}{H(z)} \right]^{\frac{1}{3}} , \quad (30)$$

that  $D_A(z)$  is the angular diameter distance. We used the fitting formula for  $z_d$  from [61] and the baryon sound speed is given by:

$$c_s(a) = \frac{1}{\sqrt{3(1 + \frac{3\Omega_b^0}{4\Omega_\gamma^0} a)}} , \quad (31)$$

where we set  $\Omega_\gamma^0 = 2.469 \times 10^{-5} h^{-2}$  [60]. The covariance matrix  $\mathbf{C}_{\text{BAO}}^{-1}$  in Eq. (27), was obtained by [60]

$$\begin{pmatrix} 4444.4 & 0. & 0. & 0. & 0. & 0. \\ 0. & 34.602 & 0. & 0. & 0. & 0. \\ 0. & 0. & 20.6611 & 0. & 0. & 0. \\ 0. & 0. & 0. & 24532.1 & -25137.7 & 12099.1 \\ 0. & 0. & 0. & -25137.7 & 134598.4 & -64783.9 \\ 0. & 0. & 0. & 12099.1 & -64783.9 & 128837.6 \end{pmatrix}.$$

The data related to cosmic microwave background, CMB, is used to study early universe and dark energy models. CMB shift parameter, is associated with the location of the first peak  $\mathbf{L}_1^{TT}$  of the CMB temperature perturbation spectrum. It provides a useful data to constrain dark energy models. The position of this peak is given by  $(l_a, R, z_*)$ , where  $R$  is the scale distance to recombination and is given for spatially flat cosmology

$$R = \sqrt{\Omega_m^0} H_0 D_A(z_*). \quad (32)$$

The quantity  $l_a$  is given by

$$l_a = \pi \frac{D_A(z_*)}{r_s(z_*)}, \quad (33)$$

and  $r_s(z)$  is the comoving sound horizon which is defined in Eq. (29). The fitted formula for  $z_*$ , the redshift of decoupling, is given in [62]. For the WMAP data set we have [60]

$$\mathbf{X}_{\text{CMB}} = \begin{pmatrix} l_a - 302.40 \\ R - 1.7264 \\ z_* - 1090.88 \end{pmatrix}. \quad (34)$$

By defining the inverse matrix

$$\mathbf{C}_{\text{CMB}}^{-1} = \begin{pmatrix} 3.182 & 18.253 & -1.429 \\ 18.253 & 11887.879 & -193.808 \\ -1.429 & -193.808 & 4.556 \end{pmatrix}, \quad (35)$$

the  $\chi_{\text{CMB}}^2$  is obtained by:

$$\chi_{\text{CMB}}^2 = \mathbf{X}_{\text{CMB}}^T \mathbf{C}_{\text{CMB}}^{-1} \mathbf{X}_{\text{CMB}}. \quad (36)$$

The observed  $H(Z)$  data, are used to constrain cosmological parameters. The advantage of using OHD is that they are acquired directly from model-independent observations. Generally Hubble parameter measurements are based on galaxy differential age and radial BAO

size methods. To avoid correlations in our calculations, we use a Hubble data catalogue that is independent to BAO measurements and includes 30 data points in the range of  $0 \leq z \leq 1.96$ , as used in [63]. The  $\chi^2$  for this data set is:

$$\chi_{\text{H}}^2 = \sum_i \frac{[H(z_i) - H_{\text{ob},i}]^2}{\sigma_i^2}. \quad (37)$$

The last data we refer to, is the growth rate data which probes structure formation on large scales. The imprint of dark energy on structure formation, made it an efficient tool for debating on dark energy models [64]. The  $f\sigma_8(z)$  data were derived from redshift space distortions, from galaxy surveys including PSCs, 2DF, VVDS, SDSS, 6dF, 2MASS, BOSS and WiggleZ. The data with their references are shown in Table. II. The  $\chi_{f\sigma_8}^2$  is written as

$$\chi_{f\sigma_8}^2 = \sum_i \frac{[f\sigma_8(z_i) - f\sigma_{8,\text{ob}}]^2}{\sigma_i^2}. \quad (38)$$

TABLE II: The  $f\sigma_8(z)$  growth data.

z	$f\sigma_8(z)$	Ref.
0.02	$0.360 \pm 0.040$	[65]
0.067	$0.423 \pm 0.055$	[66]
0.10	$0.370 \pm 0.130$	[67]
0.17	$0.510 \pm 0.060$	[68]
0.35	$0.440 \pm 0.050$	[7, 69]
0.77	$0.490 \pm 0.180$	[69, 70]
0.25	$0.351 \pm 0.058$	[71]
0.37	$0.460 \pm 0.038$	[71]
0.22	$0.420 \pm 0.070$	[72]
0.41	$0.450 \pm 0.040$	[72]
0.60	$0.430 \pm 0.040$	[72]
0.60	$0.433 \pm 0.067$	[73]
0.78	$0.380 \pm 0.040$	[72]
0.57	$0.427 \pm 0.066$	[74]
0.30	$0.407 \pm 0.055$	[73]
0.40	$0.419 \pm 0.041$	[73]
0.50	$0.427 \pm 0.043$	[73]
0.80	$0.470 \pm 0.080$	[75]

## B. Analysis

We have proceeded joint data sets, consisting of cosmological data, in order to study the models. Depending on model, there are three groups of free parameters in our analysis;

$p_1 = \{h, \Omega_m, \Omega_b, \tilde{\beta}, \tilde{\gamma}\}$ ,  $p_2 = \{h, \Omega_m, \Omega_b, \tilde{\beta}, \tilde{\gamma}, \xi\}$ ,  $p_3 = \{h, \Omega_m, \Omega_b, \tilde{\beta}, \tilde{\gamma}, n_0\}$ . Datasets are selected in a way that we can study the models in late and early universe by mixture or pure high and low redshift data. We have found the best value of the parameters and calculated chi-square  $\chi^2_{\text{tot}}$  for joint datasets. The performance of a model could be tested via the Aakaike statistical information criterion AIC. It accounts the number of degrees of freedom and the number of fitting parameters.

$$\text{AIC} = \chi^2_{\text{min}} + 2n_{\text{fit}}. \quad (39)$$

To test the effectiveness of models  $M_i$  and  $M_j$ , one considers the difference amount  $\Delta AIC_{ij} = |AIC_i - AIC_j|$ . The larger the value of  $|\Delta AIC_{ij}|$ , the higher the evidence against the model with higher value of AIC. The range  $2 \leq |\Delta AIC_{ij}| \leq 6$ , indicating a positive such evidence and for  $|AIC_{ij}| \geq 6$  a significant such evidence is concluded. Usually one of these models is the rigid  $\Lambda$ CDM model which has a good consistency with cosmological observations.

#### IV. DISCUSSION AND RESULTS

The first joint data set used in this paper is, Hubbe+SN Ia+f $\sigma_8$ +CMB+BAO. Total  $\chi^2$  for this set is written as:

$$\chi^2_{\text{tot1}} = \chi^2_{\text{Hubble}} + \chi^2_{f\sigma_8} + \chi^2_{\text{SN}} + \chi^2_{\text{BAO}} + \chi^2_{\text{CMB}}. \quad (40)$$

The results of constraint of free parameters are classified based on MGB models in Table III. The calculated  $\Delta AIC$  amounts referring to the related amount of  $\Lambda$ CDM ( $\chi^2_{\Lambda\text{CDM}}=575.205$ ). It shows that there is not any significant evidence against or in favor of  $\Lambda$ CDM for all models, since  $\Delta AIC < 6$ . However, in comparison between models, no one has a significant difference with others.

In order to investigate the cases phenomenologically, we use the best values of parameters and study the main aspects of the models.

In Fig.1, the Hubble parameters of models, are shown and compared with the data. They show acceptable treatments and explain the evolution of universe properly. In the right panel, the distance modulus of models are shown. Comparing the models with the Union data, we see that plots are clearly well fitted to the data owing to the large number of SN Ia data in the constraining process.

TABLE III: The best value parameters and their  $1-\sigma$  uncertainty for the MGB models with joint dataset1 ( $Hubbe + SNIa + f\sigma_8 + CMB + BAO$ ).

parameter	$MGB$	$IMGB$	$MGB + n_0$
$h$	$0.711978^{+0.003873}_{-0.003798}$	$0.710614^{+0.003715}_{-0.003670}$	$0.711175^{+0.003860}_{-0.003797}$
$\Omega_m^0$	$0.212647^{+0.004686}_{-0.004415}$	$0.212519^{+0.004564}_{-0.004423}$	$0.213151^{+0.003745}_{-0.003638}$
$\Omega_b^0$	$0.044142^{+0.000498}_{-0.000494}$	$0.044335^{+0.000524}_{-0.000495}$	$0.0442440^{+0.000513}_{-0.000507}$
$\tilde{\beta}$	$0.645516^{+0.000451}_{-0.000452}$	$0.642940^{+0.000441}_{-0.000442}$	$0.525705^{+0.000379}_{-0.000380}$
$\tilde{\gamma}$	$0.915838^{+0.000555}_{-0.000556}$	$0.924112^{+0.000537}_{-0.000536}$	$0.747644^{+0.000477}_{-0.000476}$
$\xi$	—	$0.303848^{+0.007741}_{-0.007966}$	—
$n_0$	—	—	$0.136901^{+0.003611}_{-0.003790}$
$\chi^2_{min}$	574.795	573.204	574.676
$\Delta AIC$	3.590	3.999	5.471

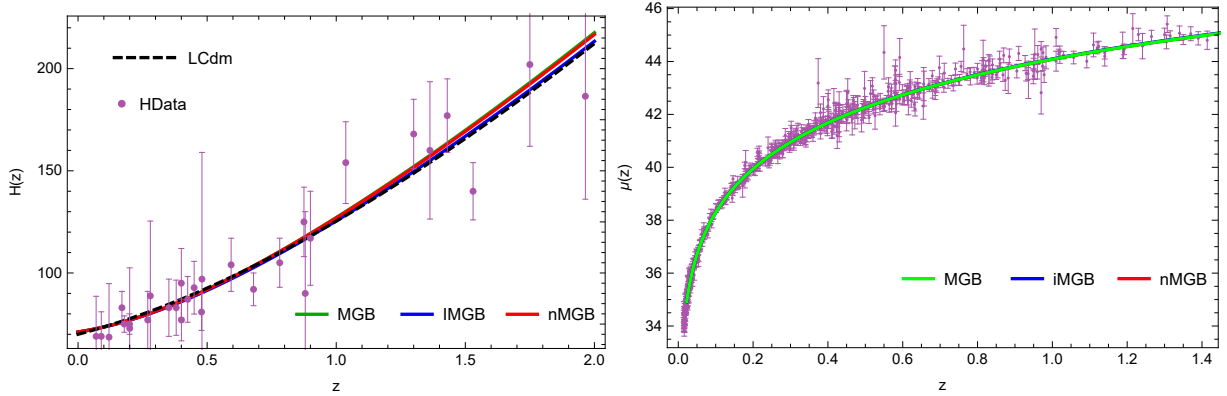


FIG. 1: Hubble parameter and luminosity distance of for MGB models with best values from data set ( $Hubbe + SNIa + f\sigma_8 + CMB + BAO$ ). Observed data are indicated with error bars.

To justify dark energy or modified gravity models, we should study them in the structure formation process. Theories with better predictions in this subject seem to be worthy to research about. In Fig.2, the density contrast and growth rate function are plotted for the models with best fit parameters from dataset ( $Hubbe + SNIa + f\sigma_8 + CMB + BAO$ ). The density contrast for IMGB model shows better competency with  $\Lambda$ CDM. In Fig.3, the  $f\sigma_8$  plots are shown. All MGB models show very close treatments. They are near to  $\Lambda$ CDM and pass through the data. In the right panel,  $\gamma$  indices for MGB like models are

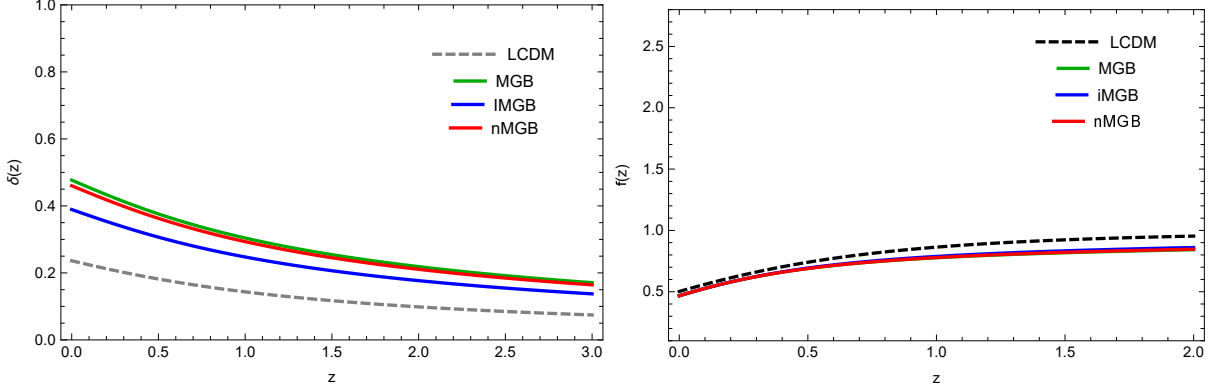


FIG. 2: The density contrast  $\delta$ , (left) and the growth rate function (right) for MGB like models with the best fit parameters from data set (*Hubble* + *SNIa* +  $f\sigma_8$  + *CMB* + *BAO*).

exhibited. The departures from  $\Lambda$ CDM index are between 2-3 percents. This may have some reasons like present experimental limits that may be alleviated by increasing the accuracy of observations.

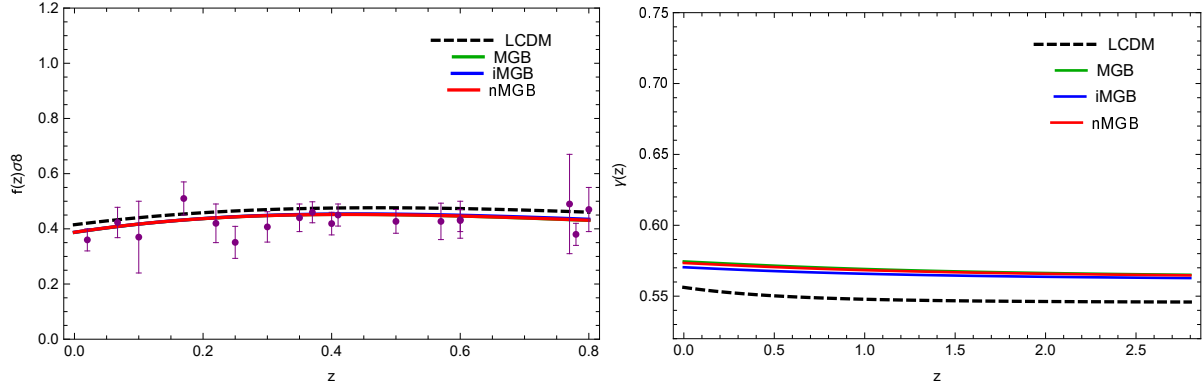


FIG. 3: The  $f\sigma_8$  plot for MGB like models, LCDM and observed data(left). The  $\gamma$  index plot for MGB like models and LCDM(right)

Generally, variety of MGB-DE models predicts the evolution of universe and structures in successful way and statistical results are satisfactory. To clarify, two more datasets are employed for late and early universe. The  $\chi^2$  for the sets are:

data set 2 (late time):

$$\chi_{\text{tot2}}^2 = \chi_{\text{Hubble}}^2 + \chi_{f\sigma_8}^2 + \chi_{\text{SN}}^2, \quad (41)$$

and data set 3 (early time):

$$\chi_{\text{tot3}}^2 = \chi_{\text{SN}}^2 + \chi_{\text{BAO}}^2 + \chi_{\text{CMB}}^2. \quad (42)$$

The results of the above combinations are summarized in Table IV. Statistically, In late universe, there is not any significant difference between mentioned models of MGB. In early universe, due to  $|\Delta AIC| > 6$ , there is a “strong” evidence against MGB models in favor of  $\Lambda$ CDM. The deduction is that, although MGB models have enough performance in late universe, it suffers to some problems at early universe. However at early time, MGB+ $n_0$  model is remarkably better than other two.

set/model	MGB	IMG	MGB+ $n_0$
$\Delta AIC_2$	0.855	1.365	2.586
$\Delta AIC_3$	14.09	12.27	6.80

TABLE IV: The comparison between AIC of models

### A. Conclusion

We have studied Modified Gauss Bonnet dark energy with main cosmological data sets. Applying the best obtained parameters to study the model, showed that all versions of MGB-DE predicts the expansion history and evolution of structures appropriately as well as  $\Lambda$ CDM. If we use pure late universe data set, we see that all versions of MGB-DE are successful in recent epoch, and there is not any significant evidence against or in favor of  $\Lambda$ CDM, whereas for early universe, statistical results indicate a significantly better agreement for  $\Lambda$ CDM as compared to all versions of MGB-DE models.

Observable show near treatments for the versions of MGB-DE. They are highly sensitive to Hubble parameter as it is predictable. The choice of data sets has a considerable effect on the outcome. Dark energy perturbations that can impress the late time expansion of the universe and evolution of structures, are ignored in this work. This case can be investigated separately.

## Acknowledgments

We would like to express sincere gratitude to Dr. Ahmad Mehrabi for constructive comments and discussion.

- 
- [1] A. G. Riess et al. (Supernova Search Team), *Astron. J.* **116**, 1009 (1998), astro-ph/9805201.
  - [2] S. Perlmutter et al. (Supernova Cosmology Project), *Nature* **391**, 51 (1998), astro-ph/9712212.
  - [3] M. Hicken, W. M. Wood-Vasey, S. Blondin, P. Challis, S. Jha, P. L. Kelly, A. Rest, and R. P. Kirshner, *Astrophys. J.* **700**, 1097 (2009), 0901.4804.
  - [4] E. Komatsu et al. (WMAP), *Astrophys. J. Suppl.* **180**, 330 (2009), 0803.0547.
  - [5] D. Larson et al., *Astrophys. J. Suppl.* **192**, 16 (2011), 1001.4635.
  - [6] K. Abazajian et al. (SDSS), *Astron. J.* **129**, 1755 (2005), astro-ph/0410239.
  - [7] M. Tegmark et al. (SDSS), *Phys. Rev.* **D74**, 123507 (2006), astro-ph/0608632.
  - [8] A. De Felice and S. Tsujikawa, *Living Rev. Rel.* **13**, 3 (2010), 1002.4928.
  - [9] T. P. Sotiriou and V. Faraoni, *Rev. Mod. Phys.* **82**, 451 (2010), 0805.1726.
  - [10] S. Nojiri and S. D. Odintsov, *Phys. Rept.* **505**, 59 (2011), 1011.0544.
  - [11] S. Nojiri and S. D. Odintsov, eConf **C0602061**, 06 (2006), [Int. J. Geom. Meth. Mod. Phys.4,115(2007)], hep-th/0601213.
  - [12] I. de Martino, M. De Laurentis, and S. Capozziello, *Universe* **1**, 123 (2015), 1507.06123.
  - [13] S. Bahamonde, C. G. Bhmer, F. S. N. Lobo, and D. Sez-Gmez, *Universe* **1**, 186 (2015), 1506.07728.
  - [14] S. Basilakos, N. E. Mavromatos, and J. Sol, *Universe* **2**, 14 (2016), 1505.04434.
  - [15] A. Khodam-Mohammadi and M. Malekjani, *Astrophys. Space Sci.* **331**, 673 (2011), 1007.2705.
  - [16] Y.-F. Cai, S. Capozziello, M. De Laurentis, and E. N. Saridakis, *Rept. Prog. Phys.* **79**, 106901 (2016), 1511.07586.
  - [17] L. Iorio, N. Radicella, and M. L. Ruggiero, *JCAP* **1508**, 021 (2015), 1505.06996.
  - [18] Y. Fujii and K. Maeda, *The scalar-tensor theory of gravitation* (Cambridge University Press, 2007), ISBN 9780521037525, 9780521811590, 9780511029882, URL <http://www.cambridge.org/uk/catalogue/catalogue.asp?isbn=0521811597>.
  - [19] V. A. Rubakov and M. E. Shaposhnikov, *Phys. Lett.* **125B**, 136 (1983).



- [20] M. Gogberashvili, *Europhys. Lett.* **49**, 396 (2000), hep-ph/9812365.
- [21] M. Gogberashvili, *Mod. Phys. Lett.* **A14**, 2025 (1999), hep-ph/9904383.
- [22] R. Maartens and K. Koyama, *Living Rev. Rel.* **13**, 5 (2010), 1004.3962.
- [23] S. Nojiri, S. D. Odintsov, and M. Sasaki, *Phys. Rev.* **D71**, 123509 (2005), hep-th/0504052.
- [24] S. Nojiri, S. D. Odintsov, and M. Sami, *Phys. Rev.* **D74**, 046004 (2006), hep-th/0605039.
- [25] S. Nojiri and S. D. Odintsov, *Phys. Lett.* **B631**, 1 (2005), hep-th/0508049.
- [26] S. Nojiri, S. D. Odintsov, and O. G. Gorbunova, *J. Phys.* **A39**, 6627 (2006), hep-th/0510183.
- [27] H. K. Jassal, J. S. Bagla, and T. Padmanabhan, *Mon. Not. Roy. Astron. Soc.* **405**, 2639 (2010), astro-ph/0601389.
- [28] K. M. Wilson, G. Chen, and B. Ratra, *Mod. Phys. Lett.* **A21**, 2197 (2006), astro-ph/0602321.
- [29] T. M. Davis et al., *Astrophys. J.* **666**, 716 (2007), astro-ph/0701510.
- [30] S. W. Allen, D. A. Rapetti, R. W. Schmidt, H. Ebeling, G. Morris, and A. C. Fabian, *Mon. Not. Roy. Astron. Soc.* **383**, 879 (2008), 0706.0033.
- [31] E. J. Copeland, M. Sami, and S. Tsujikawa, *Int. J. Mod. Phys.* **D15**, 1753 (2006), hep-th/0603057.
- [32] J. D. Bekenstein, *Phys. Rev.* **D7**, 2333 (1973).
- [33] S. Ogushi and M. Sasaki, *Prog. Theor. Phys.* **113**, 979 (2005), hep-th/0407083.
- [34] A. G. Cohen, D. B. Kaplan, and A. E. Nelson, *Phys. Rev. Lett.* **82**, 4971 (1999), hep-th/9803132.
- [35] E. N. Saridakis, *Phys. Rev.* **D97**, 064035 (2018), 1707.09331.
- [36] A. Gmez-Valent, J. Sol, and S. Basilakos, *JCAP* **1501**, 004 (2015), 1409.7048.
- [37] A. Gomez-Valent and J. Sola, *Mon. Not. Roy. Astron. Soc.* **448**, 2810 (2015), 1412.3785.
- [38] J. A. S. Lima, S. Basilakos, and J. Sola, *Mon. Not. Roy. Astron. Soc.* **431**, 923 (2013), 1209.2802.
- [39] E. L. D. Perico, J. A. S. Lima, S. Basilakos, and J. Sola, *Phys. Rev.* **D88**, 063531 (2013), 1306.0591.
- [40] S. Basilakos, J. A. S. Lima, and J. Sola, *Int. J. Mod. Phys.* **D22**, 1342008 (2013), 1307.6251.
- [41] L. E. Bleem et al. (SPT), *Astrophys. J. Suppl.* **216**, 27 (2015), 1409.0850.
- [42] J. A. S. Lima and M. Trodden, *Phys. Rev.* **D53**, 4280 (1996), astro-ph/9508049.
- [43] J. Sola, A. Gomez-Valent, and J. de Cruz Prez, *Astrophys. J.* **811**, L14 (2015), 1506.05793.
- [44] L. N. Granda, *Mod. Phys. Lett.* **A28**, 1350117 (2013), 1308.6565.

- [45] A. Khodam-Mohammadi, E. Karimkhani, and A. Alaii, Eur. Phys. J. Plus **131**, 398 (2016), 1502.07832.
- [46] E. N. Saridakis, Phys. Lett. **B661**, 335 (2008), 0712.3806.
- [47] M. Bouhmadi-Lopez, A. Errahmani, and T. Ouali, Phys. Rev. **D84**, 083508 (2011), 1104.1181.
- [48] M.-H. Belkacemi, M. Bouhmadi-Lopez, A. Errahmani, and T. Ouali, Phys. Rev. **D85**, 083503 (2012), 1112.5836.
- [49] A. Jawad, A. Pasqua, and S. Chattopadhyay, Eur. Phys. J. Plus **128**, 156 (2013), 1405.0729.
- [50] X. Zeng and W. Liu, Phys. Lett. **B726**, 481 (2013), 1305.4841.
- [51] Y.-Z. Li, S.-F. Wu, and G.-H. Yang, Phys. Rev. **D88**, 086006 (2013), 1309.3764.
- [52] T. Andrade, J. Casallerrey-Solana, and A. Ficnar, JHEP **02**, 016 (2017), 1610.08987.
- [53] L. N. Granda and D. F. Jimenez, Phys. Rev. **D90**, 123512 (2014), 1411.4203.
- [54] M. Arab and A. Khodam-Mohammadi, Eur. Phys. J. **C78**, 243 (2018), 1707.06464.
- [55] N. Suzuki et al., Astrophys. J. **746**, 85 (2012), 1105.3470.
- [56] F. Beutler, C. Blake, M. Colless, D. H. Jones, L. Staveley-Smith, L. Campbell, Q. Parker, W. Saunders, and F. Watson, Mon. Not. Roy. Astron. Soc. **416**, 3017 (2011), 1106.3366.
- [57] N. Padmanabhan, X. Xu, D. J. Eisenstein, R. Scalzo, A. J. Cuesta, K. T. Mehta, and E. Kazin, Mon. Not. Roy. Astron. Soc. **427**, 2132 (2012), 1202.0090.
- [58] L. Anderson et al., Mon. Not. Roy. Astron. Soc. **427**, 3435 (2013), 1203.6594.
- [59] C. Blake et al., Mon. Not. Roy. Astron. Soc. **418**, 1707 (2011), 1108.2635.
- [60] G. Hinshaw et al. (WMAP), Astrophys. J. Suppl. **208**, 19 (2013), 1212.5226.
- [61] D. J. Eisenstein and W. Hu, Astrophys. J. **496**, 605 (1998), astro-ph/9709112.
- [62] W. Hu and N. Sugiyama, Astrophys. J. **471**, 542 (1996), astro-ph/9510117.
- [63] J. Sol, A. Gmez-Valent, and J. de Cruz Prez, Astrophys. J. **836**, 43 (2017), 1602.02103.
- [64] P. J. E. Peebles, *Principles of physical cosmology* (Princeton University Press, Princeton, N.J, 1993), ISBN 9780691019338.
- [65] M. J. Hudson and S. J. Turnbull, Astrophys. J. **751**, L30 (2013), 1203.4814.
- [66] F. Beutler, C. Blake, M. Colless, D. H. Jones, L. Staveley-Smith, G. B. Poole, L. Campbell, Q. Parker, W. Saunders, and F. Watson, Mon. Not. Roy. Astron. Soc. **423**, 3430 (2012), 1204.4725.
- [67] M. Feix, A. Nusser, and E. Branchini, Phys. Rev. Lett. **115**, 011301 (2015), 1503.05945.
- [68] W. J. Percival et al. (2dFGRS), Mon. Not. Roy. Astron. Soc. **353**, 1201 (2004), astro-

ph/0406513.

- [69] Y.-S. Song and W. J. Percival, JCAP **0910**, 004 (2009), 0807.0810.
- [70] L. Guzzo et al., Nature **451**, 541 (2008), 0802.1944.
- [71] L. Samushia, W. J. Percival, and A. Raccanelli, Mon. Not. Roy. Astron. Soc. **420**, 2102 (2012), 1102.1014.
- [72] C. Blake et al., Mon. Not. Roy. Astron. Soc. **415**, 2876 (2011), 1104.2948.
- [73] R. Tojeiro et al., Mon. Not. Roy. Astron. Soc. **424**, 2339 (2012), 1203.6565.
- [74] B. A. Reid et al., Mon. Not. Roy. Astron. Soc. **426**, 2719 (2012), 1203.6641.
- [75] S. de la Torre et al., Astron. Astrophys. **557**, A54 (2013), 1303.2622.